JVI Journals.ASM.org

Epstein-Barr Virus Infection Induces Indoleamine 2,3-Dioxygenase Expression in Human Monocyte-Derived Macrophages through p38/Mitogen-Activated Protein Kinase and NF-κB Pathways: Impairment in T Cell Functions

Wan-li Liu,[a,b] Yue-hao Lin,[a,b] Han Xiao,[c] Shan Xing,[a,b] Hao Chen,[a,b] Pei-dong Chi,[a,b] Ge Zhang[c]

State Key Laboratory of Oncology in Southern China, Collaborative Innovation Center of Cancer Medicine, Sun Yat-sen University Cancer Center,[a] Department of Clinic Lab, Sun Yat-sen University Cancer Center,[b] and Department of Microbial and Biochemical Pharmacy, School of Pharmaceutical Sciences, Sun Yat-sen University,[c] Guangzhou, China

ABSTRACT

Epstein-Barr virus (EBV) infection has been observed in tumor-infiltrated macrophages, but its infection effects on macrophage immune functions are poorly understood. Here, we showed that some macrophages in the tumor stroma of nasopharyngeal carcinoma (NPC) tissue expressed the immunosuppressive protein indoleamine 2,3-dioxygenase (IDO) more strongly than did tumor cells. EBV infection induced mRNA, protein, and enzymatic activity of IDO in human monocyte-derived macrophages (MDMs). Infection increased the production of tumor necrosis factor alpha (TNF-α) and interleukin-6 (IL-6), whereas the neutralizing antibodies against TNF-α and IL-6 inhibited IDO induction. EBV infection also activated the mitogen-activated protein kinase (MAPK) p38 and NF-κB, and the inhibition of these two pathways with SB202190 and SN50 almost abrogated TNF-α and IL-6 production and inhibited IDO production. Moreover, the activation of IDO in response to EBV infection of MDMs suppressed the proliferation of T cells and impaired the cytotoxic activity of $CD8^+$ T cells, whereas the inhibition of IDO activity with 1-methyl-L-tryptophan (1-MT) did not affect T cell proliferation and function. These findings indicate that EBV-induced IDO expression in MDMs is substantially mediated by IL-6- and TNF-α-dependent mechanisms via the p38/MAPK and NF-κB pathways, suggesting that a possible role of EBV-mediated IDO expression in tumor stroma of NPC may be to create a microenvironment of suppressed T cell immune responses.

IMPORTANCE

$CD8^+$ cytotoxic T lymphocytes (CTLs) play an important role in the control of viral infections and destroy tumor cells. Activation of the tryptophan-catabolizing enzyme indoleamine 2,3-dioxygenase (IDO) in cancer tissues facilitates immune escape by the impairment of CTL functions. IDO expression was observed in some macrophages of the tumor stroma of nasopharyngeal carcinoma (NPC) tissue, and IDO could be induced in Epstein-Barr virus (EBV)-infected human monocyte-derived macrophages (MDMs). NPC cells and macrophages have been found to produce IDO in a gamma interferon (IFN-γ)-dependent manner. Instead, EBV-induced IDO expression in MDMs is substantially mediated by IL-6- and TNF-α-dependent mechanisms via the p38/MAPK and NF-κB pathways, which suppressed the proliferation of T cells and impaired the cytotoxic activity of $CD8^+$ T cells. This finding provides a new interpretation of the mechanism of immune escape of EBV and shows the immunosuppressive role of EBV-mediated IDO expression in tumor stroma of NPC.

Epstein-Barr virus (EBV) is a ubiquitous human virus of the herpesvirus family that is found in >90% of the world's population. Infection with EBV is associated with infectious mononucleosis and human malignancies including Burkitt's lymphoma and nasopharyngeal carcinoma (NPC) (1, 2).

EBV can infect monocytes/macrophages, intraepithelial macrophages, and Langerhans cells (3, 4). Moreover, EBV expression in macrophages infiltrating NPC, Burkitt's lymphoma, and primary lung lymphoma has also been observed (5, 6). The interaction of EBV with monocytes has been demonstrated to suppress its phagocytic activity and inhibit its potent antiviral activity (7, 8). EBV infection inhibits the development of dendritic cells by promoting the apoptosis of their monocyte precursors (9). Conversely, one study reported that EBV infection of monocytes enhanced their survival and rapidly induced their maturation into macrophages with the characteristics of potent antigen-presenting cells (APCs) (10). However, the effects of EBV infection on macrophage immune functions are poorly understood.

An immunomodulatory role for the enzyme indoleamine 2,3-dioxygenase (IDO) in macrophage functions has been suggested (11). IDO catalyzes the conversion of tryptophan into kynurenine, and altered IDO activity is often associated with pathology including neoplasia and autoimmunity (12). Several studies have described IDO-dependent T cell suppression by APCs in many infectious and inflammatory conditions, indicating that biochemical changes due to tryptophan catabolism have a profound effect

Received 15 December 2013 **Accepted** 24 March 2014
Published ahead of print 2 April 2014
Editor: R. M. Longnecker
Address correspondence to Ge Zhang, zhangge@mail.sysu.edu.cn.
W.L. and Y.L. contributed equally to this work.

doi:10.1128/JVI.03678-13

on T cell proliferation and effector functions in tissue microenvironments (13–15). IDO-mediated tryptophan metabolism, not only in APCs but also in tumor cells, represents a vital mechanism for potential T cell suppression during tumor growth (16). Our previous study indicated that exposure to the milieu created by an IDO-positive NPC cell line significantly impaired lymphocyte cytotoxicity against target tumor cells (17).

IDO expression is induced in macrophages and several other cell types under various physiological conditions, such as inflammation induced by viral and bacterial infections (18). Infection with dengue virus, HIV, poliovirus, and hepatitis C virus is associated with IDO induction in various tissues and cell types, both *in vivo* and *in vitro* (19–22). Previously reported evidence suggests that EBV infection increases the expression level of IDO in B cells and inhibits NK cell cytotoxicity (23). To date, whether IDO can be induced by EBV-infected macrophages and what effects EBV induction of IDO may have on macrophage immune functions have not been investigated.

To elucidate the potential role of IDO in macrophages during EBV infection, we investigated the signaling mechanisms by which EBV infection induces IDO expression in human monocyte-derived macrophages (MDMs) and the possible role of EBV-mediated IDO induction in creating a microenvironment of suppressed T cell immune responses in MDMs.

MATERIALS AND METHODS

Cell culture. Peripheral blood mononuclear cells (PBMCs) were isolated by Ficoll-Paque Plus gradient centrifugation of leukopacks derived from 25 healthy adult volunteers. Informed consent was obtained from the volunteers prior to participation, in accordance with the human experimentation guidelines of the Institute Research Ethics Committee of the Cancer Centre, Sun Yat-Sen University. $CD14^+$ monocytes were isolated from PBMCs by using magnetic CD14 microbeads (Miltenyi Biotech) according to the manufacturer's instructions. $CD14^+$ cells were matured into MDMs by 8 to 12 days in medium with 25 ng/ml macrophage colony-stimulating factor (M-CSF) (R&D Systems). The isolation of $CD4^+$ and $CD8^+$ T lymphocytes from PBMCs was performed by means of immunomagnetic bead separation using a Dynal CD4- or CD8-positive isolation kit (Invitrogen Dynal). The purity of $CD4^+$ and $CD8^+$ cells was >98%, as determined by flow cytometry. CNE2 (human NPC cell line) and B95-8 (EBV-positive B cell line) cells were maintained in our laboratory. All of these cells were grown in complete RPMI 1640 medium supplemented with 10% heat-inactivated fetal bovine serum (HyClone), 100 μg/ml streptomycin, and 100 U/ml penicillin under a humidified 5% CO_2 atmosphere at 37°C in a CO_2 incubator.

EBV preparation and cell treatment. EBV was purified from B95-8 cell culture supernatants as previously described (24). In brief, virus was propagated by inducing B95-8 cells with 30 ng/ml phorbol myristate acetate (PMA) and 4 mM butyric acid (both from Sigma) for 3 days. The virus was then pelleted by ultracentrifugation at 150,000 rpm for 90 min, filtered through a 0.8-mm pore size filter, and stored at −80°C. Viral titers were evaluated and adjusted to 2×10^7 transforming units (TFU)/ml. Where indicated, virus stocks were inactivated by pretreatment with 9 mJ of UV radiation with a Stratalinker instrument, which completely abolished their ability to infect cells.

For the preparation of conditioned medium (CM), MDM cells were seeded at 5×10^5 cells/ml for 24 h. Next, cells were infected with EBV or UV-irradiated EBV (UV-EBV) at various TFU/ml values for the indicated times. In certain experiments, 100 μM 1-methyl-L-tryptophan (1-MT) (Sigma-Aldrich) was added to the medium. Subsequently, the culture supernatants were harvested as CM and stored in aliquots at −80°C before use.

For antibody-blocking experiments, MDMs were preincubated with 10 μg/ml of neutralizing antibodies against tumor necrosis factor alpha (TNF-α) (mouse IgG1 [mIgG1]; eBioscience) or interleukin-6 (IL-6) (mIgG1; R&D systems) or isotype-matched control mIgG1 antibodies (eBioscience) for 1 h at 37°C before EBV infection.

For inhibitor-blocking experiments, MDMs were preincubated for 1 h at 37°C with 10 μM U0126 (MEK/extracellular signal-regulated kinase [ERK] inhibitor), 10 μM SB203580 (p38 inhibitor), 10 μM SP600125 (Jun N-terminal protein kinase [JNK] inhibitor), 0.3 μM wortmannin (phosphatidylinositol 3-kinase [PI3K] inhibitor), or 30 μM SN50 (NF-κB inhibitor). NF-κB SN50M (30 μM) (the inactive control peptide) was used as a negative control for SN50. Dimethyl sulfoxide (DSMO) was used as a vehicle control. U0126 was purchased from Cell Signaling Technology, and other reagents were obtained from Calbiochem. MDMs were subsequently infected with EBV at 0.2×10^5 TFU for 48 h.

Immunohistochemistry and immunofluorescence. Immunohistochemistry and immunofluorescence were performed by using paraffin-embedded NPC tissues or EBV-infected MDMs (EBV-MDMs). For immunohistochemistry, a rabbit polyclonal anti-IDO antibody (1:200; homemade) (17) and a mouse monoclonal anti-CD68 antibody (1:100; BD Pharmingen) were incubated with tissue sections overnight at 4°C. After washing, tissue sections were treated with biotinylated anti-mouse or anti-rabbit antibody (Zymed), followed by further incubation with the streptavidin-horseradish peroxidase (HRP) conjugate. For immunofluorescence, tissue sections or MDM cells were incubated with antibodies against IDO (1:200) or CD68-phycoerythrin (PE) (1:100; BD Pharmingen) or the serum of a NPC patient who was positive for the EBV antibody (1:100) (viral capsid antigen [VCA]-IgA titer of 1:1,280, as determined by an immunofluorescence assay) at 4°C overnight. After washing, the slides were incubated with fluorescein isothiocyanate (FITC)-conjugated secondary antibodies (1:1,000; Abcam) or Alexa Fluor 594-conjugated anti-human IgG1 antibodies (1:1,000; BD Biosciences), and the cell nuclei were stained with 4′,6-diamidino-2-phenylindole (DAPI) (Sigma). The number of $CD68^+$ and IDO^+ cells in the tumor stroma was counted. The mean values were derived from a visual analysis of 10 high-power fields (HPFs) (magnification, ×400), using a Nikon Eclipse E-200 microscope, which corresponded to an area of 0.5 mm^2 per HPF.

Flow cytometry. $CD14^+$ cells were separated from PBMCs by the use of magnetic CD14 microbeads (Miltenyi Biotech). MDMs were generated from $CD14^+$ cells in the presence of M-CSF. MDMs were infected with EBV at 0.2×10^5 TFU/ml, infected with UV-irradiated EBV, or not infected with EBV for 48 h. Cells were fixed for 10 min in 1% paraformaldehyde and then permeabilized with 1% saponin (BD Pharmingen). A FACScalibur instrument (Becton, Dickinson) and CellQuest software (Becton, Dickinson) were used for flow cytometric analysis. Monoclonal antibodies (MAbs) were obtained from BD Pharmingen, including anti-CD3-FITC, -CD4-FITC, -CD8-PE, -CD14-FITC, -CD19-PE, -CD21-FITC, -CD68-PE, -CD163-PE, and CD206-PE antibodies. The serum of a NPC patient who was positive for the EBV antibody (1:100) (VCA-IgA titer of 1:1,280, as determined by an immunofluorescence assay) and Alexa Fluor 594-conjugated goat anti-human IgG1 antibodies (BD Biosciences) were used to detect EBV infection. A rabbit polyclonal anti-IDO antibody (homemade) and goat anti-rabbit IgG1-FITC (Abcam) were used to detect IDO expression. Negative controls included isotype-matched antibodies (BD Pharmingen) and normal human serum (VCA-IgG negative, as determined by an immunofluorescence assay), which was treated as a control for detection of EBV infection.

Immunoblotting. Total protein extracts were prepared from MDM cells after treatment for the indicated time intervals. IDO was detected by using an anti-IDO polyclonal antibody (1:1,000). Mouse monoclonal antibody to EBV latent membrane protein 1 (LMP1) (1:1,000; Abcam), BZLF1 antibody (1:2,000; Millipore), and EBV nuclear antigen 1 (EBNA1) antibody (1:1,000; Santa Cruz Biotech) were used to detect EBV protein expression in MDMs. An anti-β-tubulin monoclonal antibody (1:5,000; Abcam) was used to confirm equal loading.

To examine the activation of mitogen-activated protein kinase

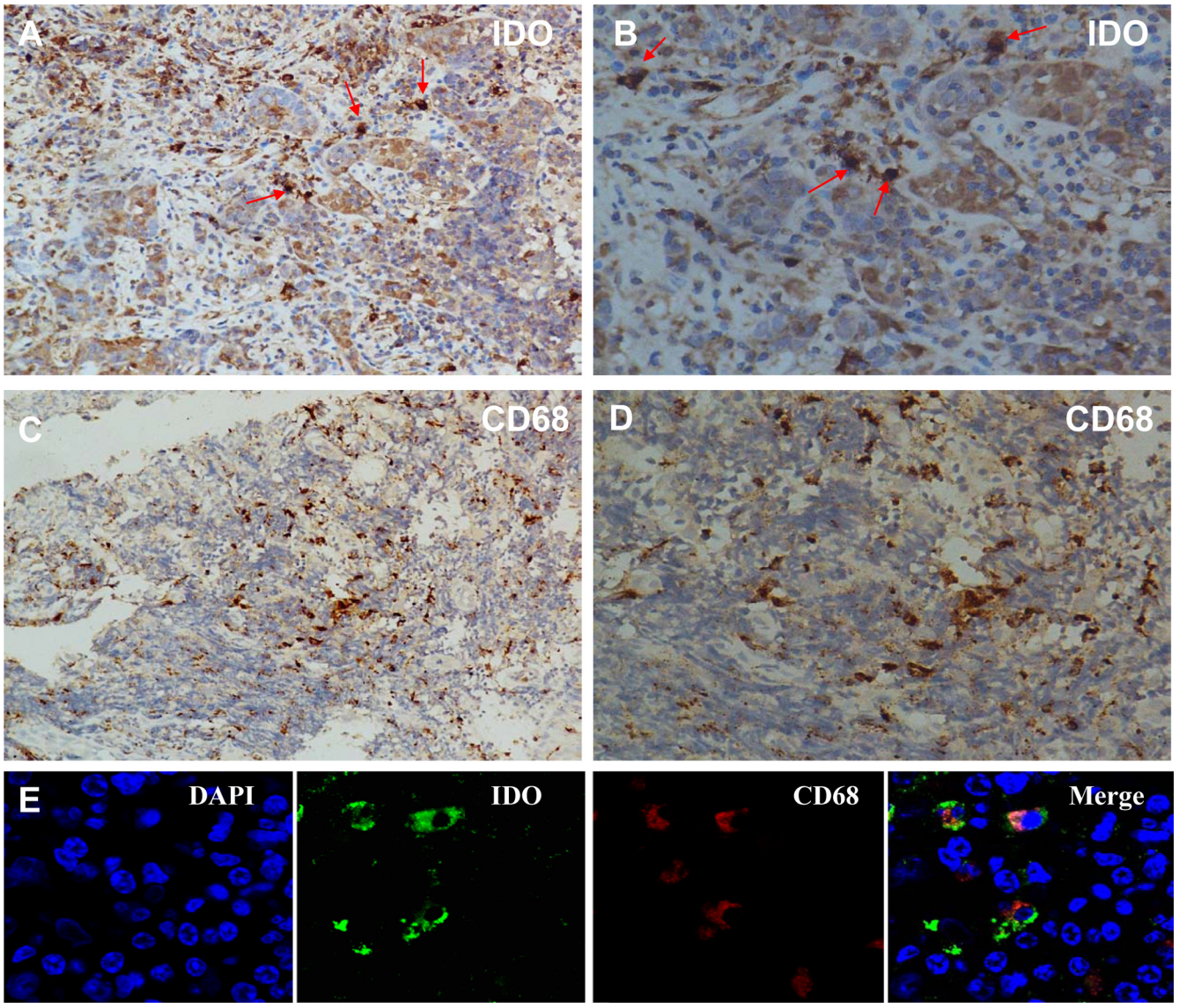

FIG 1 High IDO expression levels in macrophages from nasopharyngeal carcinoma (NPC) tissue. (A and B) Representative IDO expression in NPC tissue sections detected by immunohistochemistry (magnifications, ×200 [A] and ×400 [B]). The arrow indicates strong IDO expression in some stromal cells. (C and D) Representative CD68 expression in NPC tissue sections detected by immunohistochemistry (magnifications, ×200 [C] and ×400 [D]). (E) Representative staining of IDO (green, FITC), CD68 (red, Alexa Fluor 594), and nuclei (blue, DAPI) in NPC tumor stroma detected by coimmunofluorescence (magnification, ×1,000).

(MAPK), PI3K, and NF-κB pathways, cell lysates were prepared from MDMs infected with EBV at 2×10^5 TFU/ml or without EBV infection and probed with specific antibodies against individual components of these pathways (all antibodies were obtained from Cell Signaling). The active forms of the three MAPKs (p38, JNK, and ERK), Akt (a downstream target of PI3K), and the p65 and IκBα subunits of the NF-κB complex were detected with rabbit monoclonal antibodies to phosphorylated p38 (Thr180/Tyr1824), JNK (Thr183/Tyr185), ERK (Thr202Tyr204), Akt (Ser473), IκBα (Ser32), and NF-κB p65 (Ser536). The total amounts of MAPK, Akt, and NF-κB proteins were analyzed with rabbit monoclonal antibodies to JNK, Akt, and NF-κB p65; rabbit polyclonal antibodies to p38 and ERK; and a mouse monoclonal antibody to IκBα.

Quantitative PCR (qPCR). The total mRNA of the cells was extracted after treatment for the indicated times. First-strand cDNA synthesis was carried out by using 500 ng of total RNA. The quantification of target and reference (glyceraldehyde-3-phosphate dehydrogenase [GAPDH]) genes was performed in triplicate by using a LightCycler 480 II instrument (Roche, Applied Science). The primers used for real-time PCR were as follows: forward primer 5′-GGCAAAGGTCATGGAGATGT-3′ and reverse primer 5′-CTGCAGTCTCCATCACGAAA-3′ for IDO and forward primer 5′-GCACCGTCAAGGCTGAGAAC-3′ and reverse primer 5′-TGGTGAAGACGCCAGTGGA-3′ for GAPDH.

Measurement of IDO activity. IDO activity was assayed according to a method described previously (17). The cell culture medium was mixed with trichloroacetic acid and then centrifuged. Next, the supernatant was injected into a C_{18} column and eluted with KH_2PO_4. The concentrations of tryptophan and kynurenine were analyzed by high-performance liquid chromatography (HPLC) (Waters). Tryptophan was measured by the detection of its native fluorescence at 285-nm excitation and 365-nm emission wavelengths. Kynurenines were detected by UV absorption at the 360-nm wavelength in the same chromatographic run, and the results

were processed by using Waters Breeze software, version 3.30. IDO activity was determined by calculating the kynurenine-to-tryptophan (Kyn/Trp) ratio (μM/μM).

Cell proliferation. $CD4^+$ and $CD8^+$ T cell proliferation was assessed by a standard thymidine incorporation assay. Briefly, 1×10^5 cells were cultured in various CMs and stimulated with plate-bound anti-CD3 MAb (OKT3; ATCC) and soluble anti-CD28 MAb (BD Bioscience). After 72 h of culture, 1 μCi [^{3}H]thymidine was added, and incorporation was measured after 24 h with a β-Counter (Wallac).

EBV-specific cytotoxic T lymphocyte (CTL) assays against autologous EBV-transformed lymphoblastoid cell lines (EBV LCLs) were performed as described previously (25). Briefly, 5×10^6 to 10×10^6 PBMCs from healthy donors were used for the establishment of an EBV LCL by infection of PBMCs with concentrated supernatants from the B95-8 working cell banks. EBV LCLs were used as the target cells. To generate EBV-specific CTLs, 2×10^6 PBMCs/ml were cocultured with γ-irradiated (40 Gy) autologous EBV LCLs. After 3 consecutive restimulations, the cultures were expanded in RPMI 1640 medium containing 20 U/ml recombinant human IL-2 (rhIL-2) (R&D Systems) and 10% fetal calf serum (FCS) medium. $CD8^+$ T lymphocytes, separated from the expanded bulk CTLs by anti-CD8 MAb-precoated Dynabeads (Invitrogen Dynal), were incubated in different CMs at 37°C for 5 h just before the cell-mediated cytotoxicity assay was performed and were used as the effector cells. The cytotoxic activity of $CD8^+$ CTLs in different CMs was evaluated in a standard 4-h ^{51}Cr release assay. The effector and target cells were adjusted to effector/T cell (E/T) ratios of 40:1, 20:1, and 10:1. Cytotoxicity was quantified by the measurement of ^{51}Cr release with a gamma counter (Beckman 9000; Beckman Coulter). The percentage of specific lysis was calculated as follows: 100 × (total count/min in experimental wells − count/min of spontaneous release)/(count/min of maximum release − count/min of spontaneous release).

Cytokine analysis. The qualification of cytokines in CM was performed using a BD Cytometric Bead Array panel kit (BD Biosciences). The analytes included in the 8-plex kit were IL-1β, IL-2, IL-4, IL-6, IL-8, IL-10, gamma interferon (IFN-γ), and TNF-α. The 8 cytokines were measured by flow cytometry according to the manufacturer's instructions.

Statistical analysis. Paired *t* tests were used to analyze data, unless otherwise indicated. We report the nominal *P* value for each comparison without adjusting for multiple testing. Thus, these results should be interpreted cautiously due to the possible inflation of type 1 errors. A *P* value of <0.05 was considered to be statistically significant.

RESULTS

IDO expression in macrophages of NPC tissue. To investigate the exact expression level of IDO *in vivo*, IDO protein was detected by immunohistochemistry of paraffin-embedded archived NPC tissues. High IDO immunoreactivity was observed in NPC tissue (Fig. 1A and B). IDO localization was observed in the cytoplasm of some tumor cells. In addition, IDO staining was also observed in certain cells within the tumor stroma, and these cells exhibited stronger staining than did the cancer cells. To classify these IDO-positive cells in the tumor stroma, CD68 was detected by immunohistochemistry of NPC tissues. High CD68 expression levels were observed at the tumor stroma region (Fig. 1C and D). Furthermore, NPC tissue sections were coimmunostained with anti-IDO and anti-CD68 antibodies and visualized by immunofluorescence. As shown in Fig. 1E, in the tumor stroma, some IDO-positive cells were colocalized with CD68-positive cells by double staining. IDO-positive cells in the tumor stroma were observed in all 23 tissue samples examined. About 71.5% of $CD68^+$ cells expressed IDO protein (range, 21.2% to 89.7%) (Table 1). These assays revealed that some macrophages in the tumor stroma region of NPC tissue express IDO.

EBV infection induces IDO expression in MDMs. As macrophages in NPC tissues express IDO, we investigated whether EBV infection altered IDO expression in macrophage cells. MDMs were generated from $CD14^+$ cells, in which CD3 T cells and CD19 B cells were not detectable (Fig. 2A to C). Figure 2D to G show that the phenotype of MDMs was $CD14^{high}$ $CD163^{high}$ $CD206^{medium}$ $CD68^{positive}$. The level of CD21 expression was very low and was observed for only 2.3% of MDMs (Fig. 2H). The lytic infection protein BZLF1 and the latent infection proteins EBNA1 and LMP1 were expressed in MDMs infected with EBV, whereas none of the three proteins were found in MDMs infected with UV-irradiated EBV (UV-EBV) as well as in those without EBV infection (Fig. 2I). IDO expression in MDMs infected with EBV and UV-EBV was assessed by qPCR and Western blot analysis, respectively. The IDO mRNA and protein assays showed that IDO can be induced in MDMs by infection with live EBV but not UV-EBV (Fig. 3A to D). Infection with low-dose EBV (0.01×10^5 TFU) for 48 h was able to induce IDO expression. The IDO level was further increased in a time-dependent manner, peaking at 48 h (Fig. 3A and B), and in a dose-dependent manner, peaking at 0.2×10^5 TFU (Fig. 3C and D). The enzymatic activity of IDO was also investigated by HPLC. The enzymatic activity of IDO was almost undetectable in the supernatant of MDMs infected with UV-EBV but was observed in cells infected with EBV (Fig. 3E and F). These results are consistent with the qPCR and Western blotting results. Using an EBV-positive serum (Fig. 3G), about 54% (range, 52.1% to 56.7%) of MDMs were detected to be infected by EBV, and 47% of MDMs showed EBV infection and IDO expression by flow cytometric analysis. EBV infection and IDO expression were not detectable in MDMs infected with UV-irradiated EBV (Fig. 3H).

TABLE 1 Characteristics of nasopharyngeal carcinoma patients[a]

Characteristic	Value for nasopharyngeal carcinoma patients ($n = 23$)
No. (%) of patients of sex	
Female	4 (17.4)
Male	19 (82.6)
Median age of patients (yr) (range)	47 (19–76)
No. (%) of patients at clinical stage	
I–II	3 (13.1)
III–IV	20 (86.9)
No. (%) of patients with WHO histological classification	
NKUC	17 (73.9)
NKDC	6 (26.1)
Macrophages	
No. (%) of patients with $CD68^+$ macrophages isolated	23 (100)
Median no. of $CD68^+$ macrophages/HPF (range)	37 (14–67)
No. (%) of patients with $CD68^+$ IDO^+ macrophages isolated	23 (100)
Median no. of $CD68^+$ IDO^+ macrophages/HPF (range)	25 (6–58)
Median % $IDO^+/CD68^+$ macrophages (range)	71.5 (21.2–89.7)

[a] HPF, high-power field; WHO, World Health Organization; NKUC, nonkeratinizing undifferentiated carcinoma; NKDC, nonkeratinizing differentiated carcinoma.

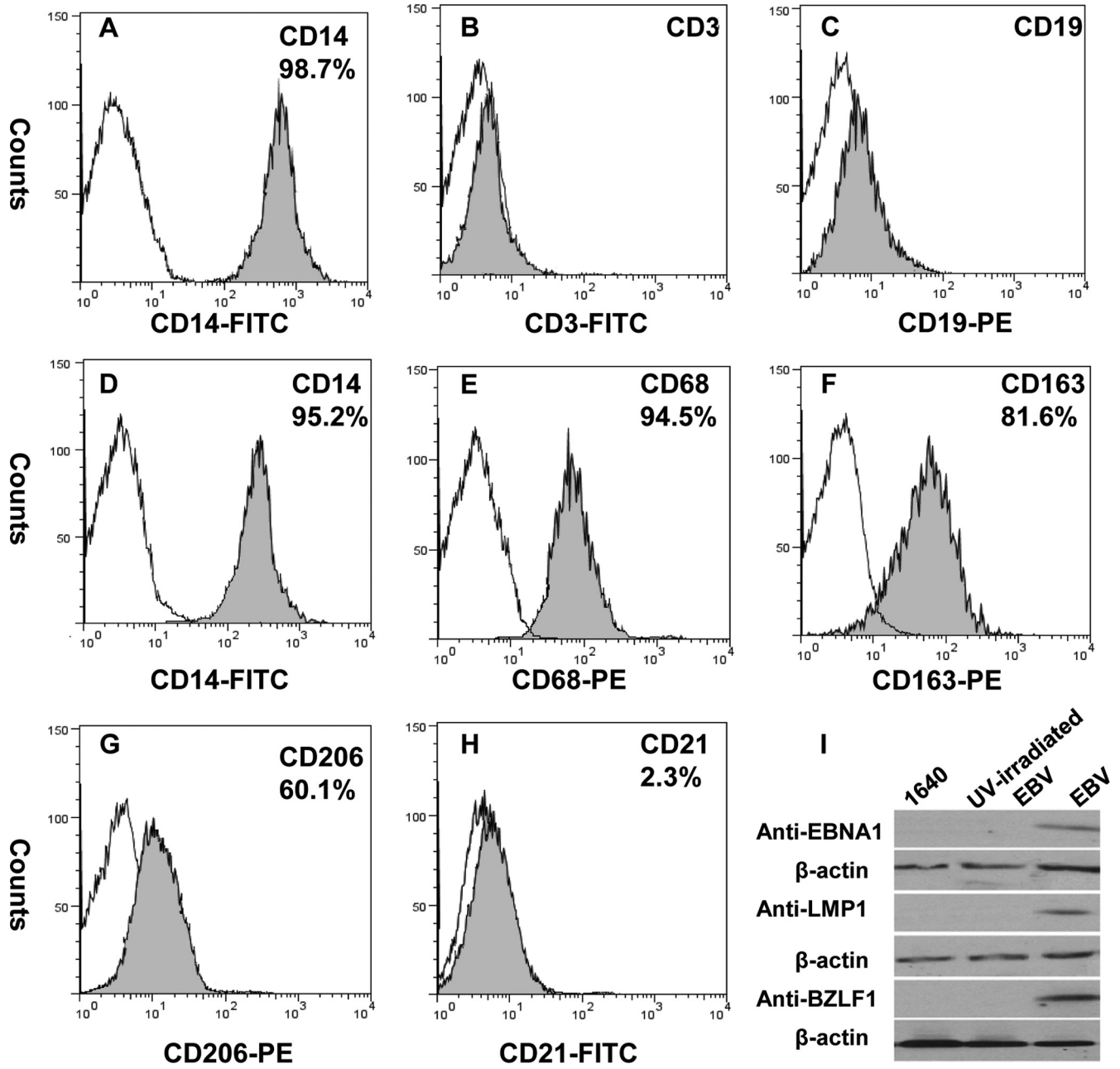

FIG 2 Purity of CD14 monocytes separated from PBMCs by magnetic CD14 microbeads. (A to C) Expression levels of CD14 (A), CD3 (B), and CD19 (C) were determined by flow cytometry. MDMs were generated in the presence of M-CSF. (D to H) Expression levels of CD14 (D), CD68 (E), CD163 (F), CD206 (G), and CD21 (H) were assessed. Gray, tested markers; white, isotype controls. Data are representative of three independent experiments. (I) Representative Western blots for EBV proteins expressed in EBV-infected MDMs. The expression levels of BZLF, LMP1, and EBNA1 in MDMs infected with EBV at 0.2×10^5 TFU/ml (EBV), infected with UV-irradiated EBV (UV-irradiated EBV), or without EBV infection (RPMI 1640 [1640]) for 48 h were assessed by Western blotting. β-Tubulin expression served as the control. Data are representative of three independent experiments, each with cells derived from a different donor.

These results confirmed that EBV infection can induce IDO expression in human MDMs.

Involvement of IL-6 and TNF-α in induction of IDO by EBV-MDMs. To investigate the cytokines that are involved in the induction of IDO in EBV-MDMs, cytokine concentrations were measured by using a cytokine bead array. As shown in Table 2, IFN-γ, IL-2, IL-4, and IL-12 concentrations in the supernatants of EBV-MDMs or MDMs infected with UV-irradiated EBV (UV-EBV-MDM) were below the limits of detection until 72 h. Low levels of IL-1β were detected in the supernatants of both EBV-MDM and UV-EBV-MDM cells, but they were not observed to be significantly different. TNF-α was detected in the supernatant of EBV-MDMs but was undetectable in control UV-EBV-MDM cells. Levels of IL-6 and IL-10 were significantly increased in the supernatant of EBV-MDMs compared to the levels in the supernatant of UV-EBV-MDMs (IL-6, 46.3 ± 5.2 versus 3.4 ± 1.2

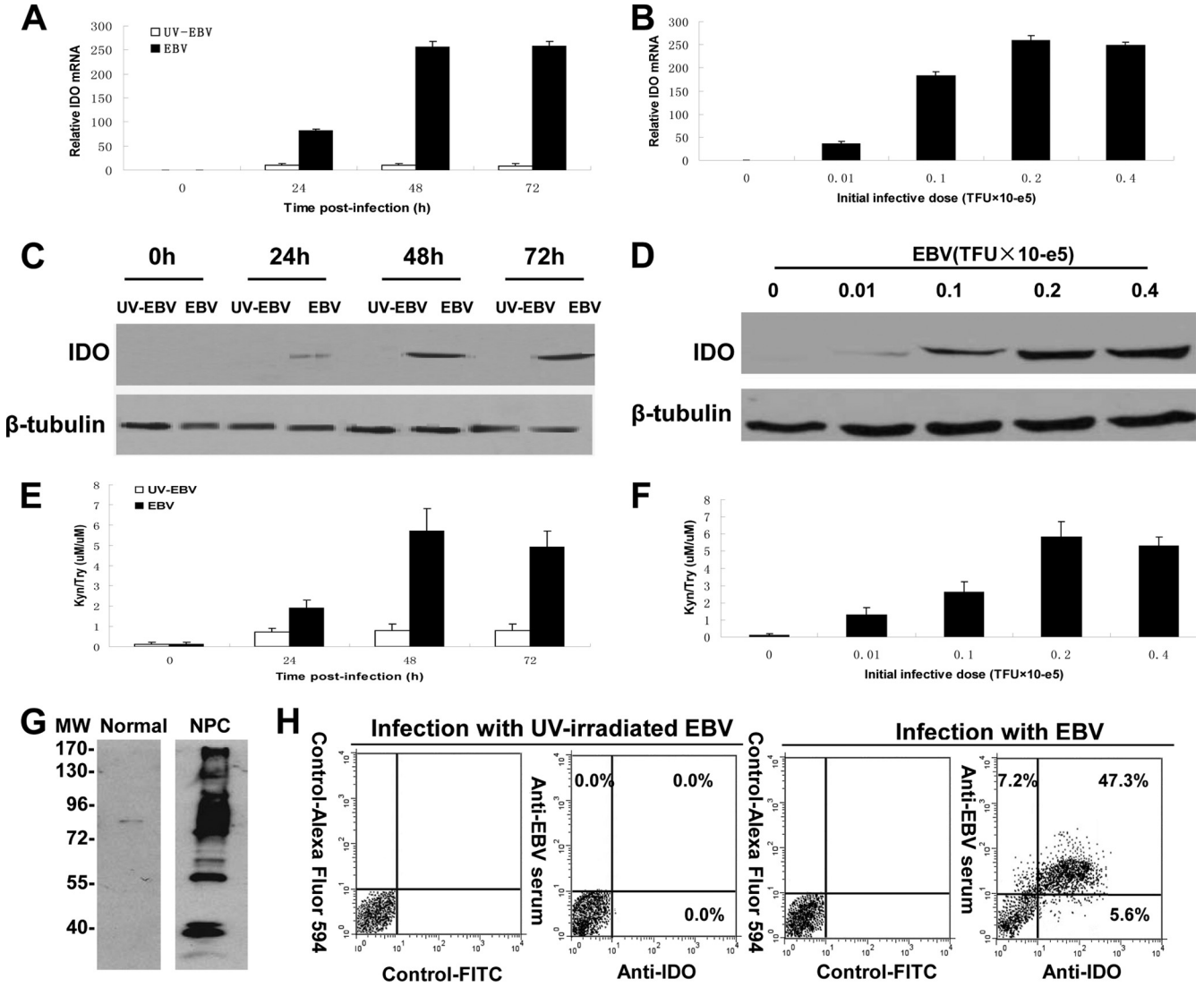

FIG 3 EBV infection induces IDO expression in monocyte-derived macrophages (MDMs). (A) IDO mRNA expression in MDMs infected with UV-irradiated EBV (UV-EBV) (white) and live EBV (EBV) (black) at 0.2×10^5 TFU/ml for 0 h, 24 h, 48 h, and 72 h, assessed by qPCR. (B) IDO mRNA expression in MDMs infected with UV-EBV or EBV for 48 h at different dosages, assessed by qPCR. (C) Representative Western blots for IDO protein expression in MDM cells infected with UV-EBV or EBV at 0.2×10^5 TFU/ml for the indicated time points. (D) Representative Western blots for IDO protein expression in MDMs infected with UV-EBV or EBV for 48 h at various dosages. (E) Induction of IDO enzymatic activity in the supernatants of MDMs infected with UV-EBV or EBV at 0.2×10^5 TFU/ml for the indicated time points. (F) Induction of IDO enzymatic activity in the supernatants of MDMs infected with UV-EBV or EBV for 48 h at various dosages. (G) Total proteins of purified EBV virions were analyzed by using a Western blot assay with EBV-positive and -negative human MW, molecular weight. (H) IDO and EBV infection were detected in MDMs infected with EBV or UV-EBV at 0.2×10^5 TFU/ml for 48 h by flow cytometry with rabbit anti-IDO antibodies and EBV-positive human serum. Rabbit IgG1 (Control-FITC) and an EBV-negative human serum (Control-Alexa Fluor 594) were used as controls. Data are representative of three independent experiments. Bars represent the means ± standard deviations of results from six donors.

pg/ml at 48 h; IL-10, 9.3 ± 1.8 versus 2.3 ± 1.1 pg/ml at 48 h [$P < 0.001$]). TNF-α levels (13.2 ± 2.4 pg/ml) and IL-6 levels (46.3 ± 5.2 pg/ml) reached their peak at 48 h post-EBV infection; the IL-6 level was substantially elevated (Fig. 4A and B). Given that TNF-α and IL-6 are potent inducers of IDO expression, we examined the possible involvement of these two cytokines in IDO expression induced by EBV infection using neutralizing antibody assays. Neutralizing antibodies against IL-6 and TNF-α significantly blocked the increased IDO expression level and enzyme activity induced by EBV-MDMs, and the combination of both antibodies almost completely blocked the induction of IDO protein and its enzyme activity (Fig. 4C and D). These data indicate that EBV infection is able to induce several proinflammatory cytokines in MDMs, with the exception of IFN-γ, and the expression of IL-6 and TNF-α mediated by EBV infection is involved in the induction of IDO.

Role of MAPK and NF-κB activation in expression of EBV-induced IDO, IL-6, and TNF-α. Activation of the MAPK, PI3K, and NF-κB signal transduction pathways is critical for IFN-γ-independent induction of IDO. We investigated whether EBV infection activates the MAPK (p38, JNK, and ERK), PI3K, and NF-κB pathways in MDMs by Western blot analysis using antibodies against the phosphorylated forms of MAPK, Akt, and NF-κB subunits. As shown in Fig. 5, live EBV rapidly induced the

TABLE 2 Levels of cytokines in supernatants of MDMs infected with EBV or UV-EBV

Cytokine	Mean cytokine concn (pg/ml) ± SD[a]									
	UV-EBV					EBV				
	0 h	12 h	24 h	48 h	72 h	0 h	12 h	24 h	48 h	72 h
IL-1β	ND	ND	0.5 ± 0.2	1.2 ± 0.5	0.9 ± 0.3	ND	ND	0.4 ± 0.2	0.9 ± 0.3	1.1 ± 0.4
IL-2	ND	ND	ND	ND	ND	ND	ND	ND	ND	ND
IL-4	ND	ND	ND	ND	ND	ND	ND	ND	ND	ND
IL-6	0.3 ± 0.2	1.1 ± 0.4	2.3 ± 0.9	3.4 ± 1.2	6.1 ± 1.7	0.3 ± 0.1	9.1 ± 1.4*	19.3 ± 3.1*	46.3 ± 5.2*	39.3 ± 3.7*
IL-10	ND	0.5 ± 0.3	1.1 ± 0.5	2.3 ± 1.1	3.1 ± 1.7	ND	1.6 ± 0.3*	4.1 ± 0.7*	9.3 ± 1.8*	8.3 ± 1.9*
IL-12	ND	ND	ND	ND	ND	ND	ND	ND	ND	ND
IFN-γ	ND	ND	ND	ND	ND	ND	ND	ND	ND	ND
TNF-α	ND	ND	ND	ND	ND	ND	1.9 ± 0.3	3.9 ± 0.4	13.2 ± 2.4	4.2 ± 0.2

[a] UV-EBV, UV-irradiated EBV; ND, not detected. Asterisks indicate a *P* value of <0.001.

phosphorylation of p38, JNK, ERK, and Akt, which generally peaked at approximately 30 to 90 min postinfection (Fig. 5A). In resting cells, the p50 and p65 heterodimers of the transcription factor NF-κB are sequestered in the cytoplasm by the IκB protein. NF-κB activation involves the phosphorylation and subsequent degradation of IκB and the phosphorylation of p65. EBV infection of MDMs led to an increase in the phosphorylation of IκBα and p65 within 30 min. Synchronously, total IκBα was degraded at between 30 and 120 min (Fig. 5B). The requirement of these pathways for the EBV-induced expression of IDO was also assessed by using specific pharmacological inhibitors. As shown in Fig. 6A, compared to the DMSO vehicle control, the p38 MAPK inhibitor

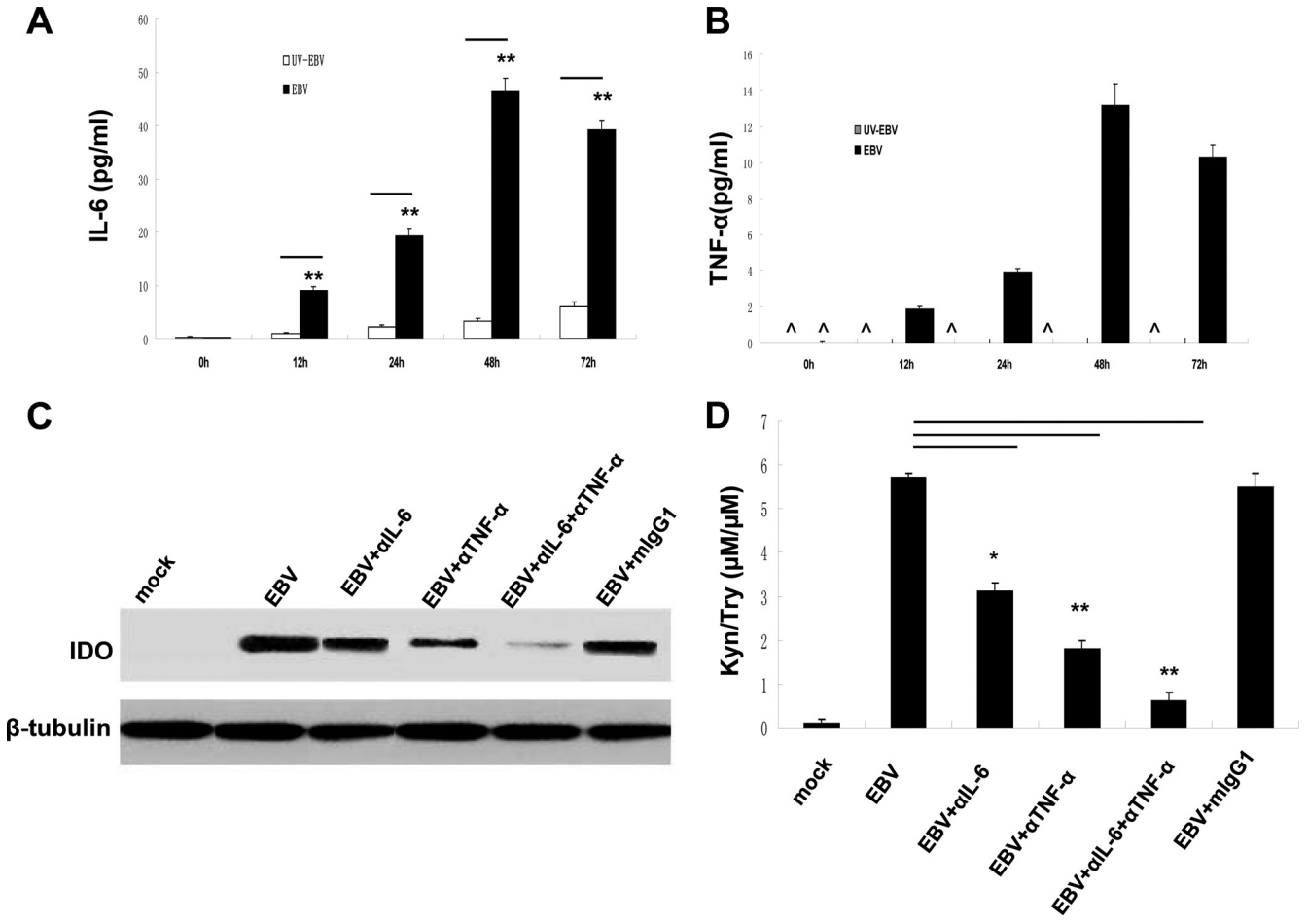

FIG 4 Involvement of IL-6 and TNF-α in induction of IDO by EBV-infected MDMs. (A and B) IL-6 (A) and TNF-α (B) levels in supernatants of EBV- or UV-EBV-infected MDMs at 0.2×10^5 TFU/ml for the indicated times. (C and D) Representative Western blots for IDO and β-tubulin in cell lysates (C) and IDO enzymatic activity in supernatants (D) of EBV-infected MDMs at 0.2×10^5 TFU/ml in the presence of neutralizing antibodies to IL-6 or TNF-α or isotype-matched mouse IgG1 (mIgG1) control antibodies for 48 h. Bars represent the means ± standard deviations of results from triplicate determinations. ∧, below the detection limit; *, $P < 0.01$; **, $P < 0.001$.

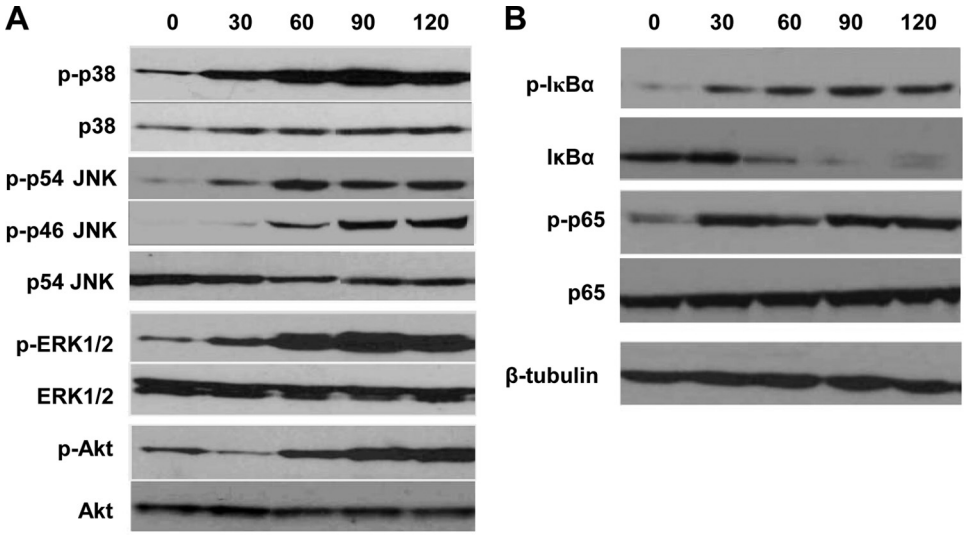

FIG 5 Activation of MAPK, PI3K, and NF-κB pathways in MDM cells infected with EBV. (A) Time course of MAPK and PI3K activation. Western blots of whole-cell lysates of MDM cells infected with EBV at 0.2×10^5 TFU/ml for various times (in minutes) were probed with antibodies to phosphorylated or total forms of MAPKs and Akt. Shown are representative Western blots of samples obtained from three donors. (B) Time course of NF-κB activation. Western blots of whole-cell lysates of MDMs infected with EBV at 0.2×10^5 TFU/ml for various periods of time were probed with antibodies against phosphorylated or total forms of IκB, p65, and β-tubulin. Shown are representative Western blots of samples obtained from three donors.

SB202190 significantly inhibited IDO mRNA expression. In contrast, The JNK inhibitor SP600125, the ERK inhibitor U0126, and the PI3K inhibitor wortmannin had little effect on IDO mRNA expression. Figure 6B and C show that SB202190 significantly inhibited IDO enzyme activity and protein production but that SP600125, U0126, and wortmannin did not. Compared to its inactive control, NF-κB SN50M, and the vehicle control, the NF-κB inhibitor SN50 significantly suppressed IDO mRNA expression, protein induction, and enzyme activities. Furthermore, the combination of SB202190 and SN50 nearly completely abolished the IDO produced by EBV-MDM cells (Fig. 6A to C). Next, we examined the effects of these inhibitors on the production of TNF-α and IL-6, respectively. SB202190 and SN50 significantly decreased the induction of TNF-α and IL-6 compared to the vehicle control. Moreover, the combination of SB202190 and SN50 nearly completely abolished the production of TNF-α and IL-6 (Fig. 6D and E). These results revealed that p38 MAPK and NF-κB activation are involved in the EBV-mediated upregulation of TNF-α and IL-6 production that, in turn, induces IDO expression in MDM cells.

IDO produced by EBV-MDM cells suppresses the proliferation of $CD4^+$ and $CD8^+$ T cells and impairs the cytolytic activity of $CD8^+$ T cells. To investigate whether the IDO produced by EBV-MDM cells can suppress the proliferation of T cells, $CD4^+$ and $CD8^+$ T cells isolated from peripheral blood mononuclear cells (PBMCs) were assessed by a standard thymidine incorporation assay. The culture medium from EBV-infected MDMs or MDMs that were not infected with EBV were harvested as conditioned medium (CM). $CD4^+$ and $CD8^+$ T cells were cultured in these CMs under anti-CD3/CD28 MAb stimulation. The levels of both $CD4^+$ and $CD8^+$ T cell proliferation were significantly lower in CM from EBV-infected MDMs than in that from uninfected MDMs (Fig. 7A and B). Next, we tested whether the observed effects of the CM from EBV-infected MDMs on $CD4^+$ and $CD8^+$ T cell proliferation rates were related to functional IDO enzyme activity. The specific IDO inhibitor 1-methyl-L-tryptophan (1-MT) was used to block enzyme activity. As shown in Fig. 7C, CM from EBV-infected MDMs had IDO enzyme activity, whereas CM from uninfected MDMs had almost undetectable IDO enzyme activity. In addition, the functional IDO enzyme activity in 1-MT-treated CM from EBV-infected MDMs was dramatically inhibited by 1-MT. When exposed to the 1-MT-treated CM of EBV-infected MDMs, the proliferation of $CD4^+$ and $CD8^+$ T cells was almost completely restored by the addition of 1-MT (Fig. 7A and B). Taken together, the data indicate that the medium collected from IDO-positive EBV-infected MDMs suppressed $CD4^+$ and $CD8^+$ T cell proliferation *in vitro*.

To investigate whether IDO produced by EBV-MDMs has an effect on the cytolytic activity of EBV-specific $CD8^+$ T cells, a standard ^{51}Cr release assay was conducted by using autologous EBV-transformed lymphoblastoid cell lines (EBV LCLs) as targets and EBV-specific $CD8^+$ T cells as effectors. EBV-specific $CD8^+$ T cells, generated from the expanded bulk CTLs by stimulation with γ-irradiated (40 Gy) autologous EBV LCLs, lysed the target cells at different E/T ratios when exposed to CM from MDMs (MDM-CM), whereas the lysis rate was remarkably reduced when the T cells were exposed to CM from EBV-MDMs. The cytolytic activity of EBV-specific $CD8^+$ T cells was effectively restored when exposed to CM from EBV-MDM cells in the presence of 1-MT (Fig. 7D). These results suggest that the inhibition of $CD8^+$ T cell-mediated cytotoxicity is attributed to IDO created by EBV-MDM, and 1-MT can abrogate this effect. These findings provide a potential role for the IDO produced by EBV-MDMs in impairing $CD8^+$ T cell cytotoxic function.

DISCUSSION

Our previous study revealed that IDO expression in NPC cells resulting from IFN-γ induction contributes to local immune tolerance in NPC (17). In the present study, higher IDO levels were observed in the tumor stroma than in the NPC tumor cells them-

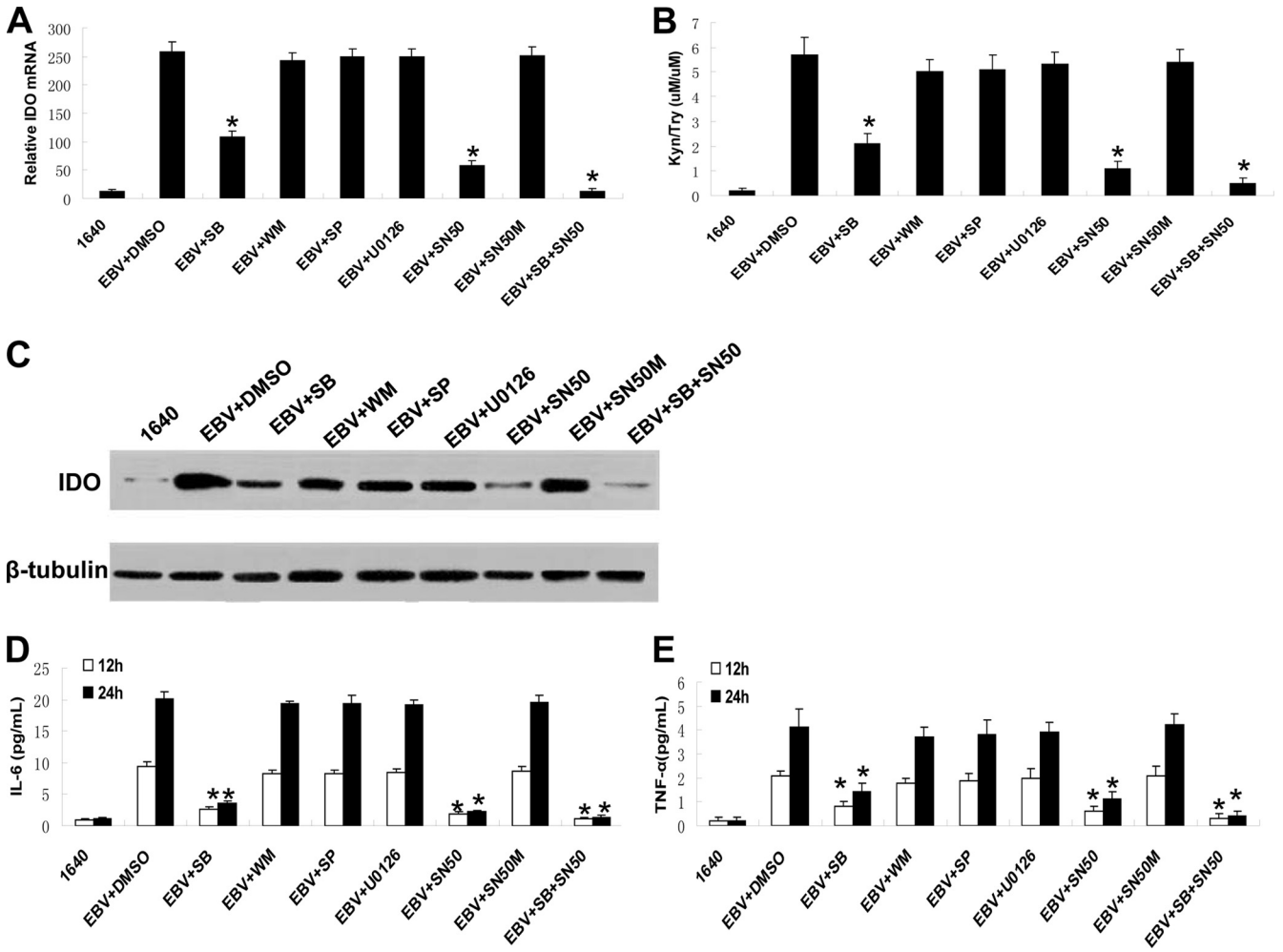

FIG 6 Role of MAPK and NF-κB activation in expression of EBV-induced IDO, IL-6, and TNF-α. MDM cells were incubated in medium (1640) (mock) or infected with EBV in the presence of SB203580 (SB) (p38 inhibitor), SP600125 (SP) (JNK inhibitor), U0126 (ERK inhibitor), the PI3K inhibitor wortmannin (WM), the NF-κB inhibitor (SN50), the NF-κB inactive control (SN50M), and the DMSO vehicle control. (A) Effects of MAPK, PI3K, and NF-κB inhibitors on IDO1 mRNA expression, determined by qPCR. (B) Effects of MAPK, PI3K, and NF-κB inhibitors on IDO enzyme activity in supernatants of EBV-infected MDMs. (C) Representative Western blots of the effects of MAPK, PI3K, and NF-κB inhibitors on IDO protein expression. (D and E) Effects of MAPK and NF-κB inhibitors on production of IL-6 (D) and TNF-α (E). Culture supernatants from MDMs infected with EBV for 12 or 24 h were assessed for the accumulation of IL-6 ($n = 5$) and TNF-α ($n = 5$). Bars represent the means ± standard deviations of results from three independent experiments. *, $P < 0.001$ compared to the vehicle control.

selves. Given that viral infection can induce IDO expression in macrophages and that EBV-infected macrophages have been observed in NPC tissues, we then asked whether EBV infection of macrophages can induce IDO expression. Indeed, we found that EBV infection does induce IDO expression in MDMs but that irradiated EBV cannot. These data suggested that EBV infection is a potent inducer of IDO expression in MDMs.

In most cell types, IDO is induced in response to specific inflammatory stimuli. IFN-γ represents the principal IDO inducer, and other inflammatory stimuli also induce IDO, including TNF-α, IL-6, IL-1β, and lipopolysaccharide (LPS), although markedly less than IFN-γ (26–29). In the present study, TNF-α synergized with IL-6 to mediate IDO induction in EBV-MDMs and did not necessarily require the synthesis of IFN-γ. In line with our results, several microbial infections of MDMs have been reported to upregulate IDO expression in a TNF-α-dependent manner but not in an IFN-γ-dependent manner, including HIV, West Nile virus (WNV), *Haemophilus ducreyi*, and *Listeria monocytogenes* infections (20, 30–32). Synergistic activation of IDO by IL-1β, TNF-α, and IL-6 in human monocytic THP-1 cells exposed to LPS was reported previously (28). Recently, IL-6 was shown to directly upregulate IDO expression in both Neuro-2a cells and an organotypic hippocampal tissue culture (33). In addition, our data indicate that a combination of anti-TNF-α and anti-IL-6 antibodies did not completely abolish the IDO production induced by EBV infection, supporting the possible involvement of additional molecules.

TNF-α-mediated activation of IDO through the MAPK/p38 and NF-κB pathways has been reported for microbial infections (29–32, 34). Our data indicate that EBV induces IDO expression in response to TNF-α and IL-6 stimuli in MDMs dominantly though the activation of the MAPK/p38 and NF-κB pathways. These results are consistent with previous studies that described HIV-induced IDO expression in dendritic cells and WNV-in-

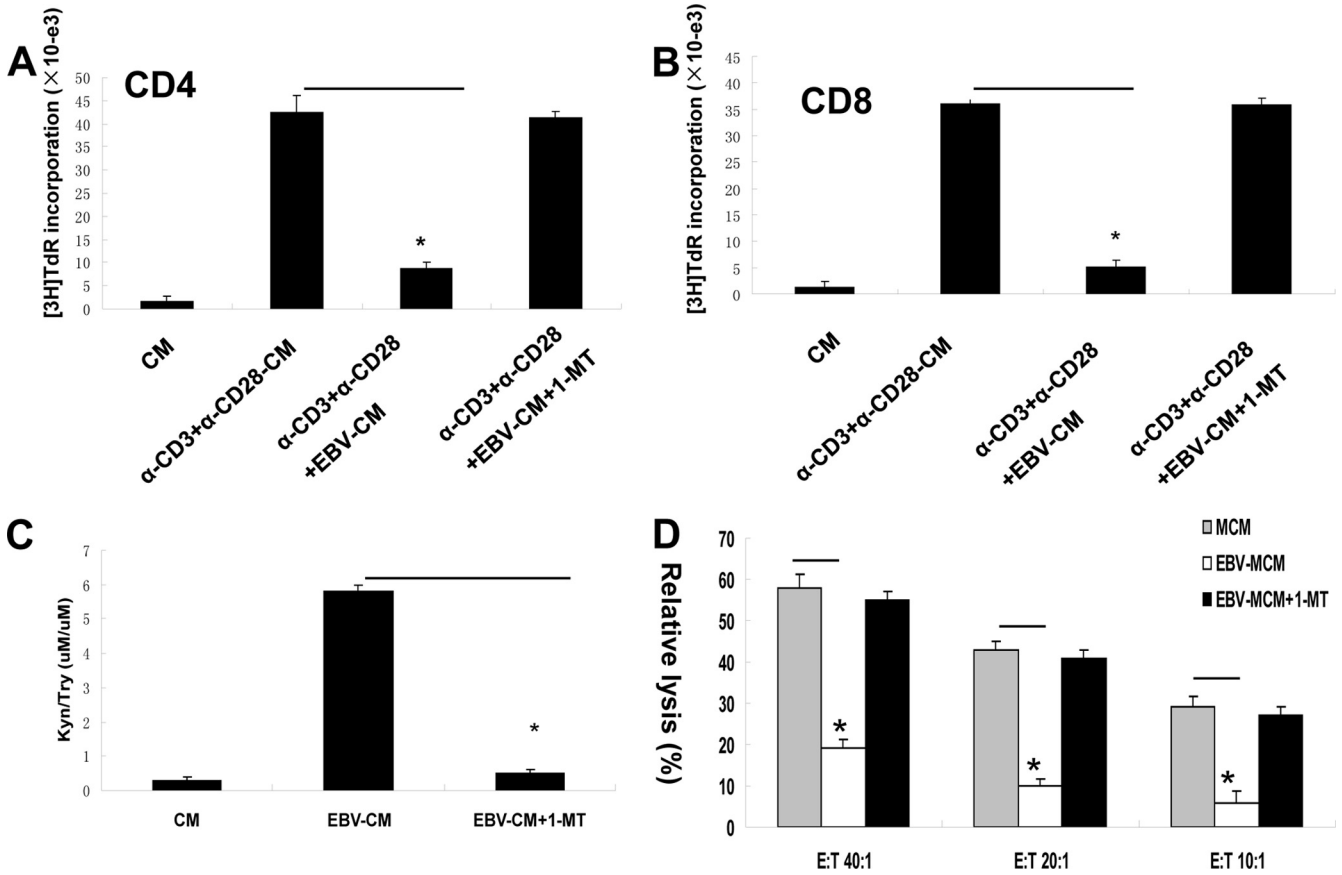

FIG 7 Effects of IDO in conditional medium (CM) of EBV-MDMs on proliferation of $CD4^+$ T cells and $CD8^+$ T cells, and cytolytic activity of $CD8^+$ T cells. (A and B) Representative [^{3}H]thymidine ([^{3}H]TdR) incorporation proliferation assay of $CD4^+$ T cells (A) and $CD8^+$ T cells (B) derived from PBMCs in CM of MDM cells infected or not with EBV by coactivation with anti-CD3/CD28 antibodies. (C) Concentrations of kynurenine and tryptophan in the supernatants of MDMs infected with EBV at 0.2×10^5 TFU/ml (EBV-CM), without EBV infection (CM), or infected with EBV and treated with 1-MT (100 μM) (EBV-CM + 1MT) for 48 h, as measured by HPLC. (D) Effects of IDO on cytotoxic activity of EBV-specific CD8 CTLs against target cell EBV LCLs. EBV-specific CD8 CTLs were cultured in the CM of EBV-infected MDMs at 0.2×10^5 TFU/ml (EBV-CM), uninfected MDMs (CM), or MDMs infected with EBV and treated with 1-MT (100 μM) (EBV-CM + 1MT) for 48 h. Cytolytic activity against the target cells was evaluated by using a standard ^{51}Cr release assay. The E/T ratios are indicated. Bars represent the means ± standard deviations of results from three independent experiments. *, $P < 0.001$.

duced IDO expression in MDMs that predominantly depended on the activation of the MAPK/p38 and NF-κB pathways (20, 30). It has been confirmed that EBV infection activates the PI3K, JNK, and MAPK/p38 pathways and both the canonical and noncanonical NF-κB signaling pathways (35–37). Activation of the p38, JNK, ERK, and NF-κB pathways leads to the production of IDO-inducing cytokines such as TNF-α and IL-6, which act in an autocrine manner to stimulate the MAPK and NF-κB pathways. The MAPK and NF-κB pathways contribute to IDO induction indirectly by promoting the production of TNF-α and directly by regulating IDO gene promoter activity, in which transcriptional factors, such as AP-1, NF-κB, and NF–IL-6, are known to be activated by TNF-α and IL-6 (28).

IDO expression in APCs and tumor cells can potently inhibit the immune response (38, 39). It is therefore plausible that active IDO, expressed in MDMs after EBV infection, acts to create an immunosuppressive microenvironment. This mechanism may be one of the mechanisms by which NPC cells evade the immune response. Our data show that exposure to the microenvironment created by IDO-positive MDM cells severely suppressed both $CD4^+$ and $CD8^+$ T cell proliferation. These results favor a model describing the proliferation arrest of T cells by IDO (39). In addition, we have presented evidence that the exposure to IDO-expressing CM from EBV-MDMs dramatically weakened the cytolytic function of $CD8^+$ T cells, derived from PBMCs, against target cells. In accordance with our observations, Liu et al. reported that in an experimental rat lung allograft model, IDO creates a local microenvironment that leads to not only a reduction in the numbers of $CD8^+$ tumor-infiltrating lymphocytes (TILs) but also the loss of the cytotoxic activity of the $CD8^+$ effector T cells toward their target cells (40). The impaired cytotoxic function observed for IDO-treated $CD8^+$ T cells was accompanied by defects in the production of granule cytotoxic proteins, including perforin and granzymes A and B. Moreover, IDO leads to an impaired bioenergetic condition in active $CD8^+$ T cells via the selective inhibition of complex I in the mitochondrial electron transfer chain (40). Our previous study also showed that exposure to the milieu created by IDO-positive tumor cells, including NPC cells and esophageal tumor cells, significantly impaired lymphocytes against target tumor cells (17, 41). Although IDO was induced by tumor cells and stromal macrophages in NPC tissue through different mechanisms, the production of IDO from both of them together con-

tributed to the immune-suppressive microenvironment, which might downregulate anti-EBV or antitumor T cell responses, leading to EBV persistence or tumor immune evasion. However, further studies are needed to elucidate the exact mechanisms by which IDO expression in EBV-infected MDMs reduces the cytotoxicity of $CD8^+$ T cells.

Taken together, these findings indicate that TNF-α and IL-6 are upregulated by MDMs in response to EBV infection and that these two cytokines synergistically mediate the induction of IDO expression. EBV-induced IDO expression in MDMs is mediated largely by the p38/MAPK and NF-κB pathways. The activation of IDO in response to EBV infection of MDMs could be a key event in creating an immunosuppressive microenvironment by suppressing the proliferation of T cells and impairing the cytotoxic function of $CD8^+$ T cells. Although the precise role of tumoral IDO in EBV-MDMs remains to be elucidated, our findings suggest that blocking IDO activity may provide a means of restoring host antivirus and antitumour immunity in the treatment of NPC.

ACKNOWLEDGMENTS

This work was supported by the National Natural Science Foundation of China (grant no. 30972762) and the 973 Program (grant no. 2011CB504800).

REFERENCES

1. **Tao Q, Young LS, Woodman CB, Murray PG.** 2006. Epstein-Barr virus (EBV) and its associated human cancers—genetics, epigenetics, pathobiology and novel therapeutics. Front. Biosci. **11:**2672–2713. http://dx.doi.org/10.2741/2000.
2. **Xu ZJ, Zheng RS, Zhang SW, Zou XN, Chen WQ.** 2013. Nasopharyngeal carcinoma incidence and mortality in China in 2009. Chin. J. Cancer **32:**453–460. http://dx.doi.org/10.5732/cjc.013.10118.
3. **Tugizov S, Herrera R, Veluppillai P, Greenspan J, Greenspan D, Palefsky JM.** 2007. Epstein-Barr virus (EBV)-infected monocytes facilitate dissemination of EBV within the oral mucosal epithelium. J. Virol. **81:**5484–5496. http://dx.doi.org/10.1128/JVI.00171-07.
4. **Walling DM, Ray AJ, Nichols JE, Flaitz CM, Nichols CM.** 2007. Epstein-Barr virus infection of Langerhans cell precursors as a mechanism of oral epithelial entry, persistence, and reactivation. J. Virol. **81:**7249–7268. http://dx.doi.org/10.1128/JVI.02754-06.
5. **Shimakage M, Sakamoto H.** 2010. Macrophage involvement in Epstein-Barr virus-related tumors. Exp. Ther. Med. **1:**285–291. http://dx.doi.org/10.3892/etm_00000044.
6. **Shimakage M, Sakamoto H, Harada S, Sasagawa T, Kodama K.** 2007. Expression of the Epstein-Barr virus in lymphoproliferative diseases of the lung. Oncol. Rep. **17:**1347–1352. http://dx.doi.org/10.3892/or.17.6.1347.
7. **Savard M, Bélanger C, Tremblay MJ, Dumais N, Flamand L, Borgeat P, Gosselin J.** 2000. EBV suppresses prostaglandin E2 biosynthesis in human monocytes. J. Immunol. **164:**6467–6473. http://www.jimmunol.org/content/164/12/6467.long.
8. **Savard M, Belanger C, Tardif M, Gourde P, Flamand L, Gosselin J.** 2000. Infection of primary human monocytes by Epstein-Barr virus. J. Virol. **74:**2612–2619. http://dx.doi.org/10.1128/JVI.74.6.2612-2619.2000.
9. **Li L, Liu D, Hutt-Fletcher L, Morgan A, Masucci MG, Levitsky V.** 2002. Epstein-Barr virus inhibits the development of dendritic cells by promoting apoptosis of their monocyte precursors in the presence of granulocyte macrophage-colony-stimulating factor and interleukin-4. Blood **99:**3725–3734. http://dx.doi.org/10.1182/blood.V99.10.3725.
10. **Salek-Ardakani S, Lyons SA, Arrand JR.** 2004. Epstein-Barr virus promotes human monocyte survival and maturation through a paracrine induction of IFN-alpha. J. Immunol. **173:**321–331. http://www.jimmunol.org/content/173/1/321.long.
11. **Johnson TS, Munn DH.** 2012. Host indoleamine 2,3-dioxygenase: contribution to systemic acquired tumor tolerance. Immunol. Invest. **41:**765–797. http://dx.doi.org/10.3109/08820139.2012.689405.
12. **Munn DH, Mellor AL.** 2007. Indoleamine 2,3-dioxygenase and tumor-induced tolerance. J. Clin. Invest. **117:**1147–1154. http://dx.doi.org/10.1172/JCI31178.
13. **Munn DH, Mellor AL.** 2003. Macrophages and the regulation of self-reactive T cells. Curr. Pharm. Des. **9:**257–264. http://dx.doi.org/10.2174/1381612033392026.
14. **Fallarino F, Grohmann U, Vacca C, Orabona C, Spreca A, Fioretti MC, Puccetti P.** 2003. T cell apoptosis by kynurenines. Adv. Exp. Med. Biol. **527:**183–190. http://dx.doi.org/10.1007/978-1-4615-0135-0_21.
15. **de Souza Sales J, Lara FA, Amadeu TP, de Oliveira Fulco T, da Costa Nery JA, Sampaio EP, Pinheiro RO, Sarno EN.** 2011. The role of indoleamine 2,3-dioxygenase in lepromatous leprosy immunosuppression. Clin. Exp. Immunol. **165:**251–263. http://dx.doi.org/10.1111/j.1365-2249.2011.04412.x.
16. **Katz JB, Muller AJ, Prendergast GC.** 2008. Indoleamine 2,3-dioxygenase in T-cell tolerance and tumoral immune escape. Immunol. Rev. **222:**206–221. http://dx.doi.org/10.1111/j.1600-065X.2008.00610.x.
17. **Liu P, Xie BL, Cai SH, He YW, Zhang G, Yi YM, Du J.** 2009. Expression of indoleamine 2,3-dioxygenase in nasopharyngeal carcinoma impairs the cytolytic function of peripheral blood lymphocytes. BMC Cancer **9:**416. http://dx.doi.org/10.1186/1471-2407-9-416.
18. **Zelante T, Fallarino F, Bistoni F, Puccetti P, Romani L.** 2009. Indoleamine 2,3-dioxygenase in infection: the paradox of an evasive strategy that benefits the host. Microbes Infect. **11:**133–141. http://dx.doi.org/10.1016/j.micinf.2008.10.007.
19. **Becerra A, Warke RV, Xhaja K, Evans B, Evans J, Martin K, de Bosch N, Rothman AL, Bosch I.** 2009. Increased activity of indoleamine 2,3-dioxygenase in serum from acutely infected dengue patients linked to γ interferon antiviral function. J. Gen. Virol. **90:**810–817. http://dx.doi.org/10.1099/vir.0.004416-0.
20. **Boasso A, Herbeuval JP, Hardy AW, Anderson SA, Dolan MJ, Fuchs D, Shearer GM.** 2007. HIV inhibits CD4+ T-cell proliferation by inducing indoleamine 2,3-dioxygenase in plasmacytoid dendritic cells. Blood **109:**3351–3359. http://dx.doi.org/10.1182/blood-2006-07-034785.
21. **Heyes MP, Saito K, Jacobowitz D, Markey SP, Takikawa O, Vickers JH.** 1992. Poliovirus induces indoleamine-2,3-dioxygenase and quinolinic acid synthesis in macaque brain. FASEB J. **6:**2977–2989.
22. **Larrea E, Riezu-Boj JI, Gil-Guerrero L, Casares N, Aldabe R, Sarobe P, Civeira MP, Heeney JL, Rollier C, Verstrepen B, Wakita T, Borrás-Cuesta F, Lasarte JJ, Prieto J.** 2007. Upregulation of indoleamine 2,3-dioxygenase in hepatitis C virus infection. J. Virol. **81:**3662–3666. http://dx.doi.org/10.1128/JVI.02248-06.
23. **Song H, Park H, Kim J, Park G, Kim YS, Kim SM, Kim D, Seo SK, Lee HK, Cho D, Hur D.** 2011. IDO metabolite produced by EBV-transformed B cells inhibits surface expression of NKG2D in NK cells via the c-Jun N-terminal kinase (JNK) pathway. Immunol. Lett. **136:**187–193. http://dx.doi.org/10.1016/j.imlet.2011.01.009.
24. **Moss DJ, Pope JH.** 1972. Assay of the infectivity of Epstein-Barr virus by transformation of human leucocytes in vitro. J. Gen. Virol. **17:**233–236. http://dx.doi.org/10.1099/0022-1317-17-2-233.
25. **Smith CA, Ng CY, Heslop HE, Holladay MS, Richardson S, Turner EV, Loftin SK, Li C, Brenner MK, Rooney CM.** 1995. Production of genetically modified Epstein-Barr virus-specific cytotoxic T cells for adoptive transfer to patients at high risk of EBV-associated lymphoproliferative disease. J. Hematother. **4:**73–79. http://dx.doi.org/10.1089/scd.1.1995.4.73.
26. **Murakami Y, Hoshi M, Imamura Y, Arioka Y, Yamamoto Y, Saito K.** 2013. Remarkable role of indoleamine 2,3-dioxygenase and tryptophan metabolites in infectious diseases: potential role in macrophage-mediated inflammatory diseases. Mediators Inflamm. **2013:**391984. http://dx.doi.org/10.1155/2013/391984.
27. **Fujigaki S, Saito K, Sekikawa K, Tone S, Takikawa O, Fujii H, Wada H, Noma A, Seishima M.** 2001. Lipopolysaccharide induction of indoleamine 2,3-dioxygenase is mediated dominantly by an IFN-gamma-independent mechanism. Eur. J. Immunol. **31:**2313–2318. http://dx.doi.org/10.1002/1521-4141(200108)31:8<2313::AID-IMMU2313>3.0.CO;2-S.
28. **Fujigaki H, Saito K, Fujigaki S, Takemura M, Sudo K, Ishiguro H, Seishima M.** 2006. The signal transducer and activator of transcription 1alpha and interferon regulatory factor 1 are not essential for the induction of indoleamine 2,3-dioxygenase by lipopolysaccharide: involvement of p38 mitogen-activated protein kinase and nuclear factor-kappaB pathways, and synergistic effect of several proinflammatory cytokines. J. Biochem. **139:**655–662. http://dx.doi.org/10.1093/jb/mvj072.
29. **Prendergast GC, Chang MY, Mandik-Nayak L, Metz R, Muller AJ.** 2011. Indoleamine 2,3-dioxygenase as a modifier of pathogenic inflammation in cancer and other inflammation-associated diseases. Curr. Med. Chem. **18:**2257–2262. http://dx.doi.org/10.2174/092986711795656072.

30. **Yeung AW, Wu W, Freewan M, Stocker R, King NJ, Thomas SR.** 2012. Flavivirus infection induces indoleamine 2,3-dioxygenase in human monocyte-derived macrophages via tumor necrosis factor and NF-κB. J. Leukoc. Biol. **91:**657–666. http://dx.doi.org/10.1189/jlb.1011532.
31. **Li W, Katz BP, Spinola SM.** 2011. Haemophilus ducreyi lipooligosaccharides induce expression of the immunosuppressive enzyme indoleamine 2,3-dioxygenase via type I interferons and tumor necrosis factor alpha in human dendritic cells. Infect. Immun. **79:**3338–3347. http://dx.doi.org/10.1128/IAI.05021-11.
32. **Popov A, Abdullah Z, Wickenhauser C, Saric T, Driesen J, Hanisch FG, Domann E, Raven EL, Dehus O, Hermann C, Eggle D, Debey S, Chakraborty T, Krönke M, Utermöhlen O, Schultze JL.** 2006. Indoleamine 2,3-dioxygenase-expressing dendritic cells form suppurative granulomas following Listeria monocytogenes infection. J. Clin. Invest. **116:**3160–3170. http://dx.doi.org/10.1172/JCI28996.
33. **Kim H, Chen L, Lim G, Sung B, Wang S, McCabe MF, Rusanescu G, Yang L, Tian Y, Mao J.** 2012. Brain indoleamine 2,3-dioxygenase contributes to the comorbidity of pain and depression. J. Clin. Invest. **122:**2940–2954. http://dx.doi.org/10.1172/JCI61884.
34. **Fu X, Lawson MA, Kelley KW, Dantzer R.** 2011. HIV-1 Tat activates indoleamine 2,3 dioxygenase in murine organotypic hippocampal slice cultures in a p38 mitogen-activated protein kinase-dependent manner. J. Neuroinflammation **8:**88. http://dx.doi.org/10.1186/1742-2094-8-88.
35. **Vaysberg M, Hatton O, Lambert SL, Snow AL, Wong B, Krams SM, Martinez OM.** 2008. Tumor-derived variants of Epstein-Barr virus latent membrane protein 1 induce sustained Erk activation and c-Fos. J. Biol. Chem. **283:**36573–36585. http://dx.doi.org/10.1074/jbc.M802968200.
36. **Dawson CW, Laverick L, Morris MA, Tramoutanis G, Young LS.** 2008. Epstein-Barr virus-encoded LMP1 regulates epithelial cell motility and invasion via the ERK-MAPK pathway. J. Virol. **82:**3654–3664. http://dx.doi.org/10.1128/JVI.01888-07.
37. **Yoshizaki T, Kondo S, Wakisaka N, Murono S, Endo K, Sugimoto H, Nakanishi S, Tsuji A, Ito M.** 2013. Pathogenic role of Epstein-Barr virus latent membrane protein-1 in the development of nasopharyngeal carcinoma. Cancer Lett. **337:**1–7. http://dx.doi.org/10.1016/j.canlet.2013.05.018.
38. **Uyttenhove C, Pilotte L, Théate I, Stroobant V, Colau D, Parmentier N, Boon T, Van den Eynde BJ.** 2003. Evidence for a tumoral immune resistance mechanism based on tryptophan degradation by indoleamine 2,3-dioxygenase. Nat. Med. **9:**1269–1274. http://dx.doi.org/10.1038/nm934.
39. **Mellor AL, Keskin DB, Johnson T, Chandler P, Munn DH.** 2002. Cells expressing indoleamine 2,3-dioxygenase inhibit T cell responses. J. Immunol. **168:**3771–3776. http://www.jimmunol.org/content/168/8/3771.long.
40. **Liu H, Liu L, Liu K, Bizargity P, Hancock WW, Visner GA.** 2009. Reduced cytotoxic function of effector CD8+ T cells is responsible for indoleamine 2,3-dioxygenase-dependent immune suppression. J. Immunol. **183:**1022–1031. http://dx.doi.org/10.4049/jimmunol.0900408.
41. **Zhang G, Liu WL, Zhang L, Wang JY, Kuang MH, Liu P, Lin YH, Dai SQ, Du J.** 2011. Involvement of indoleamine 2,3-dioxygenase in impairing tumor-infiltrating CD8 T-cell functions in esophageal squamous cell carcinoma. Clin. Dev. Immunol. **2011:**384726. http://dx.doi.org/10.1155/2011/384726.